Elsevier Editorial System(tm) for Radiography

Manuscript Draft

Manuscript Number:

Title: Modifications to mobile chest radiography technique during the COVID-19 pandemic - implications of X-raying through side room windows

Article Type: Full Length Article

Keywords: COVID-19, mobile radiography, modified technique, image quality, radiation dose.

Corresponding Author: Dr. Andrew England, B.Sc (Hons); M.Sc; PhD

Corresponding Author's Institution: Keele University

First Author: Andrew England, B.Sc (Hons); M.Sc; PhD

Order of Authors: Andrew England, B.Sc (Hons); M.Sc; PhD; Emily Littler, BSc (Hons); Simon Romani, PhD; Philip Cosson, DProf

Suggested Reviewers: Peter Hogg MPhil
Professor of Radiography, University of Salford
p.hogg@salford.ac.uk
Experience in COVID-19 related imaging and phantom based research.

Cover Letter

Dr Andrew England

Senior Lecturer in Radiography

Keele University

Stafforshire

UK

26 June 2020

Dear Professor Nightingale,

Modifications to mobile chest radiography technique during the COVID-19 pandemic – implications of X-raying through side room windows

I am writing in support of our submission on an Original Research article to Radiography. I can confirm that this is original work and has not been published in or submitted to any other journal. The work reported in this manuscript is a phantom based experiment and as such does not request institution review board approval. All authors are aware of this submission.

If you require any further information, please let me know?

Andrew England

a.england@keele.ac.uk

*Title Page (with author details)

Modifications to mobile chest radiography technique during the COVID-19 pandemic – implications of X-raying through side room windows

Andrew England, PhD – School of Allied Health Professions, Keele University, Staffordshire, UK.
Emily Littler, BSc (Hons) – Department of Radiology, Warrington and Halton Teaching Hospitals NHS Foundation Trust, Warrington, UK.
Simon Romani, PhD – LPD Lab Services, Blackburn, UK.
Philip Cosson, DProf – Medical Imaging Department, Teesside University, Middlesbrough, UK.

Corresponding author: Dr Andrew England, Mackay Building, School of Allied Health Professions, Keele University, Staffordshire, UK (a.england@keele.ac.uk)

*Abstract

ABSTRACT

Purpose: Modifications to common radiographic techniques have resulted from the challenges presented by the COVID-19 pandemic. Reports exist regarding the potential benefits of undertaking mobile radiography through side room windows. The aim of this study was to evaluate the impact on image quality and exposure factors when undertaking such examinations.

Methods: A phantom based study was undertaken using a digital X-ray room. Control acquisitions, using a commercially available image quality test tool, were performed using standard mobile chest radiography acquisition factors. Image quality (physical and visual), incidence surface air kerma (ISAK), Exposure Index (EI) and Deviation Index (DI) were recorded. Image quality and radiation dose were further assessed for two additional (experimental) scenarios, where a side room window was located immediately adjacent to the exit port of the light beam diaphragm. The goal of experimental scenario one was to modify exposure factors to maintain the control ISAK. The goal of experimental scenario two was to modify exposure factors to maintain the control EI and DI. Dose and image quality data were compared between the three scenarios.

Results: To maintain the pre-window (control) ISAK (76 μGy), tube output needed a three-fold increase (90 kV / 4 mAs versus 90 kV / 11.25 mAs). To maintain EI /DI a more modest increase in tube output was required (90 kV / 8 mAs / ISAK 54 μGy). Physical and visual assessments of spatial resolution and signal-to-noise ratio were indifferent between the three scenarios. There was a slight statistically significant reduction in contrast-to-noise ratio when imaging through the glass window (2.3 versus 1.4 and 1.2; P=0.005).

Conclusions: Undertaking mobile X-ray examinations through side room windows is potentially feasible but does require an increase in tube output and is likely to be limited by minor reductions in image quality.

Implications for Practice: Mobile examinations performed through side room windows should only be used in limited circumstances and future clinical evaluation of this technique are warranted.

KEYWORDS

COVID-19, mobile radiography, modified technique, image quality, radiation dose.

INTRODUCTION

A number of institutions are reporting that in some instances mobile chest radiography is being undertaken through side room windows[1] in order to prevent the spread of the novel coronavirus SARS-CoV-2 (**Figure 1**). Such practices are likely to provide additional opportunities for infection prevention but may also induce some limitations. Image quality degradation resulting from increased X-ray beam filtration, additional implications for radiation protection and increased wear and tear on the X-ray unit are just a few of the potential issues.

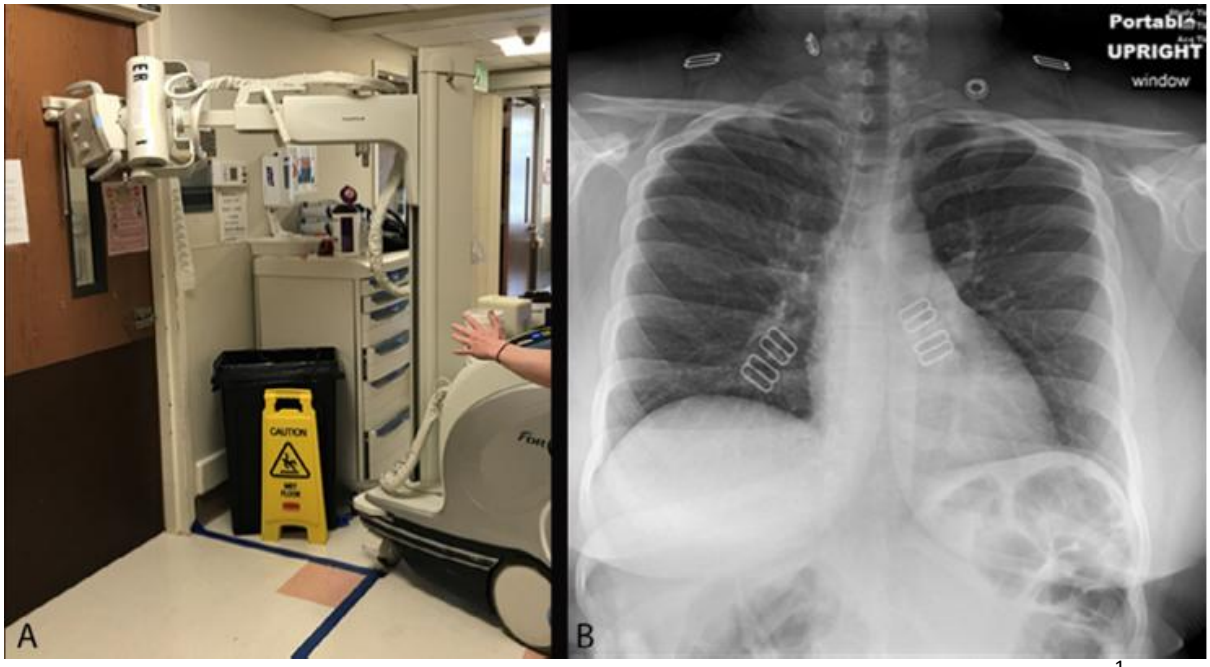

Figure 1. Example of a mobile CXR examination being undertaken through glass[1]. The mobile DR machine is positioned outside of the isolation (side room), Image A. Image B the resultant AP CXR image.

Aim

To evaluate the effect on image quality, radiation dose and tube life of undertaking X-ray examinations through glass side room windows.

MATERIALS AND METHODS

This experimental study was conducted using a commercially available fixed digital radiography unit and all images were acquired using a commercially available quality control test tool. As a result, ethics committee approval was not required but permission from the departmental manager was obtained.

Preliminary simulation

The experiment was at first simulated to provide starting values, to visualise the effect on the X-ray beam spectrum, and to estimate the effect on the filament current thus ensuring no damage to the equipment was possible. TechnicVR v2.0 (Shaderware Ltd, UK) was used to provide the simulated data.

Imaging equipment and technique

Prior to commencing the study, quality assurance testing was undertaken in accordance with IPEM Report 91[2]; results were within expected tolerances. A Samsung XGEO GC80 digital general radiography system (Samsung, Seoul, South Korea) together with a Caesium Iodide (CsI) AeroDR image detector (Konica Minolta Medical Imaging USA Inc, Wayne, NJ) was used. The image receptor had an image capture area of 35 x 43 cm with a 1994 x 2430-pixel matrix, pixel size was 175 µm.

A Leeds Test Objects TOR 18FG (Leeds Test Objects, Leeds, UK) test tool was positioned erect 180 cm away from the X-ray tube focal spot (**Figure 2A**). A fixed collimation field, at the detector surface, of 10 x 10 cm was applied. Beam centring was at the midpoint of the TOR 18FG test tool (**Figure 2B**) and six degrees of caudal tube angulation was applied. as would typically be applied during erect anteroposterior chest radiography[3].

An isolation / side room window was simulated using a double-glazed unit suitable for use as a door insert (**Figure 2C**). The insert considered of two panes of 4 mm tempered glass separated by a 30 mm void and could be standard insert for an commercial interior door.

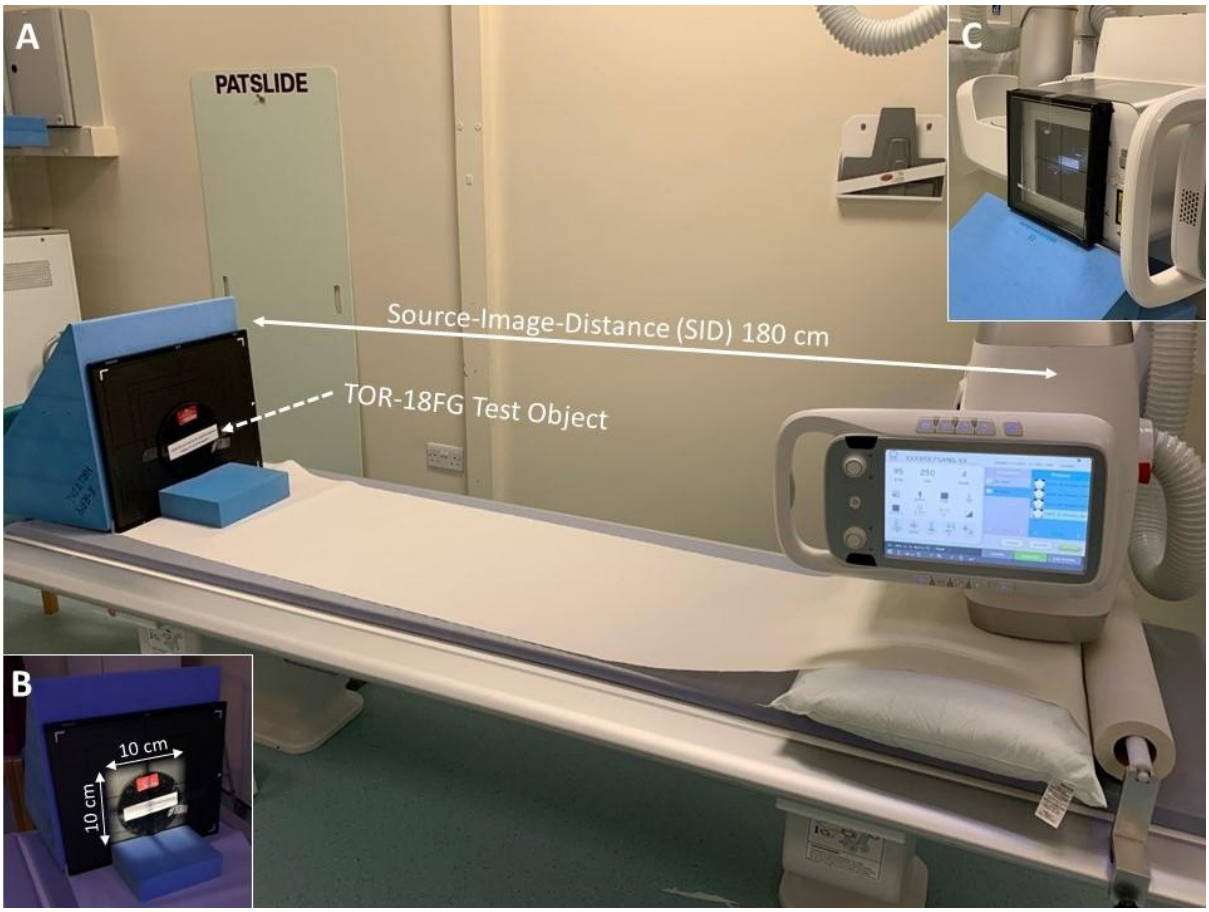

Figure 2. Experimental setup of the digital X-ray unit (A) and the TOR-18FG test object (B). For some acquisitions, a glass window unit (200 x 200 x 28 mm) was placed directly in contact with the exit port of the light beam diaphragm (C).

The control series of acquisitions consisted of a fixed SID, filament size, tube potential and total filtration in keeping with mobile chest radiography. The tube charge was then selected to achieve an incident surface air kerma (ISAK) sufficient to report a zero

deviation index (DI). The experimental series of acquisitions included the glass window and an incremental increase in tube charge was used to produce an ISAK equivalent to the control. The final experimental condition was a tube charge that resulted in a zero DI / equivalent EI to the control acquisitions.

Dosimetry

Three exposures were performed for each experimental setup. To minimise random errors from occurring, three exposures and three Dose Area Product (DAP), DI, EI and ISAK values were recorded.

Image quality assessment

Both physical and visual grading of the resultant image quality was undertaken. Both methods used images displayed using a picture archiving and communication system (PACS) workstation (Carestream Vue PACS Version 12.2.2.1025, Carestream Health, Rochester, NY) and a 23 inch 2-megapixel colour monitor (Dell UZ2315H, Dell, Austin, TX). For each image the spatial resolution was determined together with the number of high contrast low detail discs visible on the image by a human observer. Observers were permitted to change the magnification and window levels in order to maximise visualisation, reflecting typical clinical processes of image interpretation. Observers consisted of two qualified radiographers with clinical experience ranging from 4 to 24 years. All observers were blinded to the image acquisition parameters, the presence or absence of the glass window and each other's observations. Room lighting was dimmed and reflected a typical radiology reporting room.

Signal to noise ratio (SNR) and contrast to noise ratio (CNR) have been successfully used as image quality metrics in a number of similar studies[4-7]. Four region of interests (ROIs) were drawn in homogenous structures on the resultant test object images (**Figure 3**). These were chosen to represent a range of low contrast details starting for the highest to the lowest and included the 7th and 11th discs. In order to sample the mean and standard deviation of the pixel values on the images software on the PACS workstation (Carestream Vue PACS) was used. SNR and CNR were calculated according to the following equations[8,9]:

$$SNR = \frac{mean\ signal}{\sigma_{noise}}$$

$$CNR = \frac{ROI_X - ROI_B}{\sigma_2}$$

where ROI_X is the mean signal from the area of interest (TOR contrast disc) and ROI_B is the mean signal from the background noise. σ_2 was calculated as $\sqrt{(SD1)^2 + (SD2)^2/2}$ where SD1 and SD2 and the standard deviations for ROI_x and ROI_B.

In terms of spatial resolution, the resultant image from the TOR-18FG test object was evaluated using three computer generated line profiles (**Figure 4**). By summating the number of line pairs that were visible (four clear peaks and troughs on the histogram) the resolution of the image could be determined.

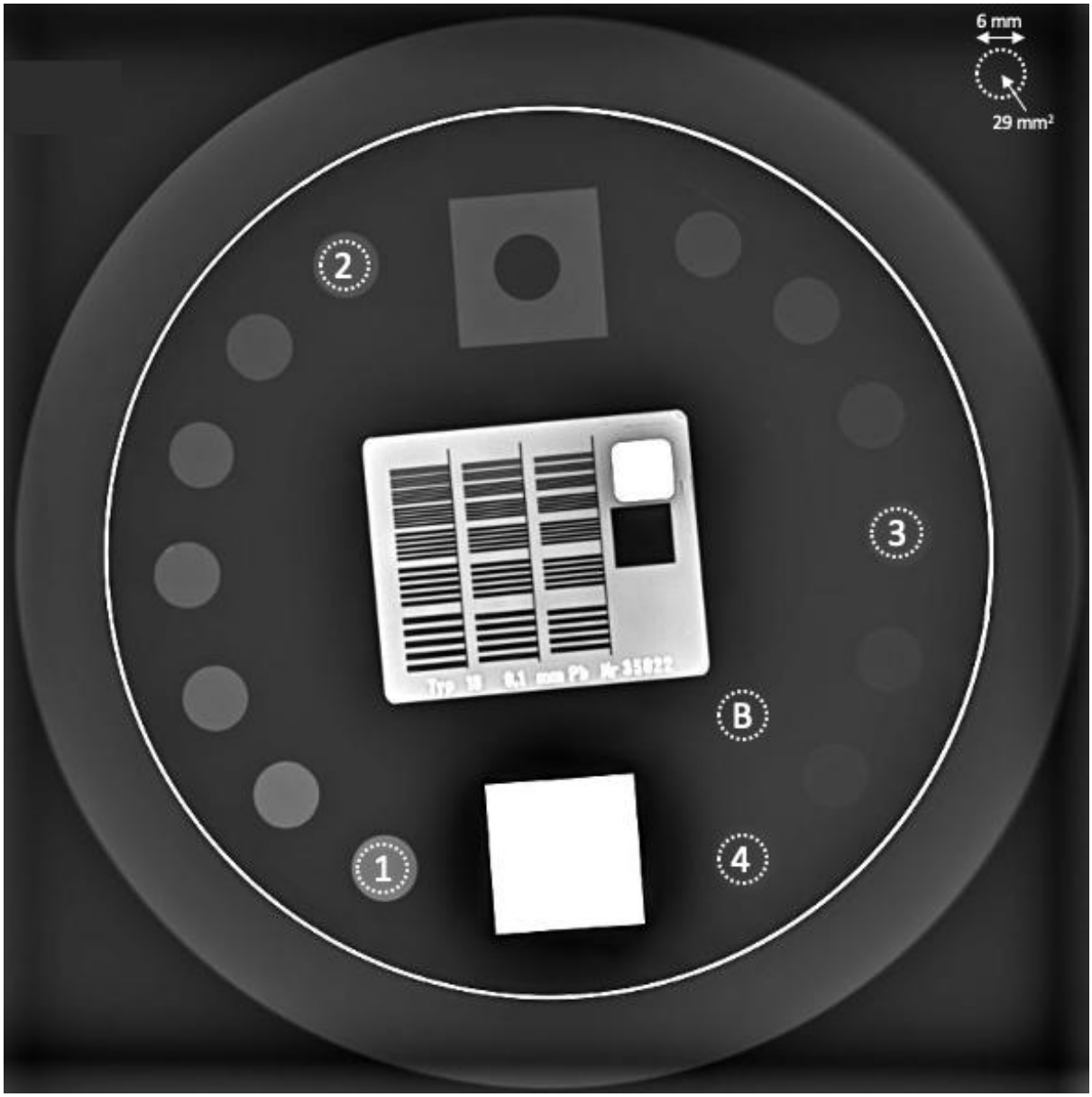

Figure 3. Resultant TOR-18FG test object image indicating the four ROI positions (1-4) and the location for measuring background signal and noise (B). All ROIs were located in the same position between measurements and had a diameter of 6 mm and an area of 29 mm^2.

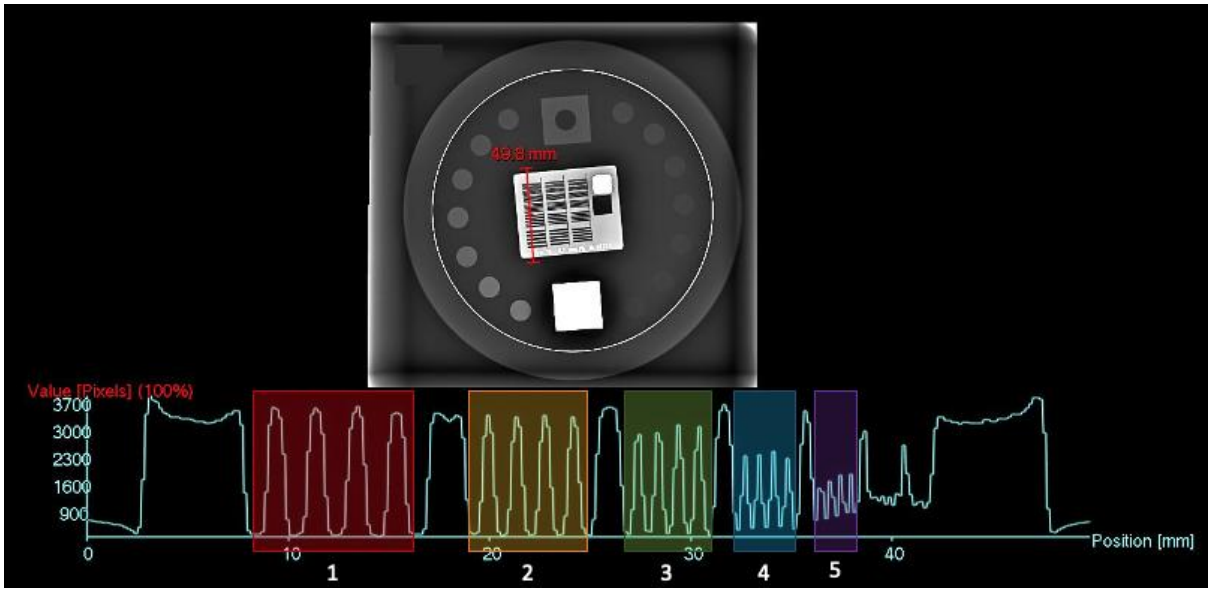

Figure 4. Resultant TOR-18FG test object image. A 50 mm straight line profile has been plotted across the first column of line pairs. Using the resultant histogram, the number of clear pairs of four lines are calculated. In this example, four groups of line pairs are visible where by four clear peaks and troughs were identifiable (coloured boxes).

Statistical analysis

Data were inputted into Microsoft Excel (Microsoft Inc, Redmond, WA) and analysis was undertaken using the statistical programming package R. For each image acquisition a series of calculations were made for SNR, CNR and spatial resolution. Scenarios were compared using ANOVA and Tukey's HSD post-hoc analysis. Data were also summarised as a series of tables and graphs. P values of less than 0.05 were considered significant.

RESULTS

Tube filtration was 3.5 mm Al, the focal spot size used was 1.2 mm^2, no additional filtration was included, SID was 180cm and tube voltage was 90kV. For all acquisitions the target exposure index was 127. In the control condition (absence of the glass window), the tube charge necessary to generate a DI of zero was 4 mAs. This resulted in a mean (SD) ISAK and EI of 75.9 (0.2) μGy and 128.0 (0.6), respectively.

The initial simulation using the same fixed exposure parameters and a tube charge of 4mAs (achieved from a tube current of 250mA and exposure time of 16ms) resulted in an ISAK of 75.9 μGy and a Receptor Incident Air Kerma (RIAK) of 55.9 uGy (the TOR-18FG test object was substituted for 10mm of PMMA and 0.1mm of Al). The simulation generated an incident surface spectrum with an HVL of 4.6 mm Al. The filament current was 5.2 Amps (**Figure 5**). The simulation predicted a reduction in ISAK and RIAK to 35.2 μGy and 26.7 μGy respectively with the addition of 8 mm of glass (**Figure 5**). To maintain a similar RIAK to the control with glass in the primary beam, the tube charge would need to increase to 8 mAs. This could either be achieved from a tube current of 250mA and exposure time of 33ms (filament current of 5.2 Amps), or from a tube current of 500mA and an exposure time of 16ms (filament current of 5.6 Amps). This X-ray beam, after transit through the glass, would have an HVL of 6.0 mm Al **(Figure 6)**.

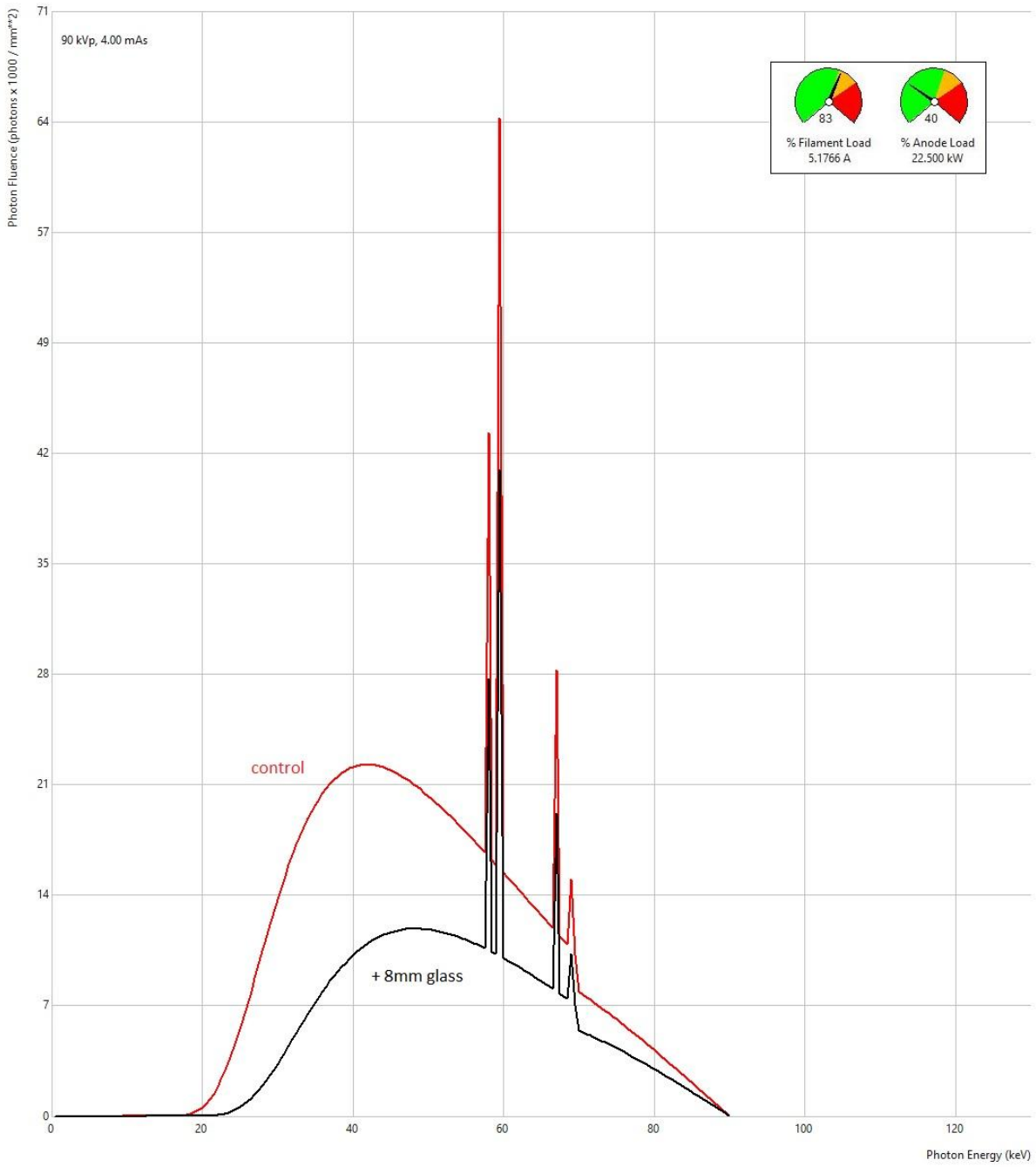

Figure 5. TechnicVR v2.0 (Shaderware Ltd, UK) simulation of the X-ray spectrum of the control beam (red line) and the required filament current (insert). The black line represents the beam attenuated by 8mm of glass.

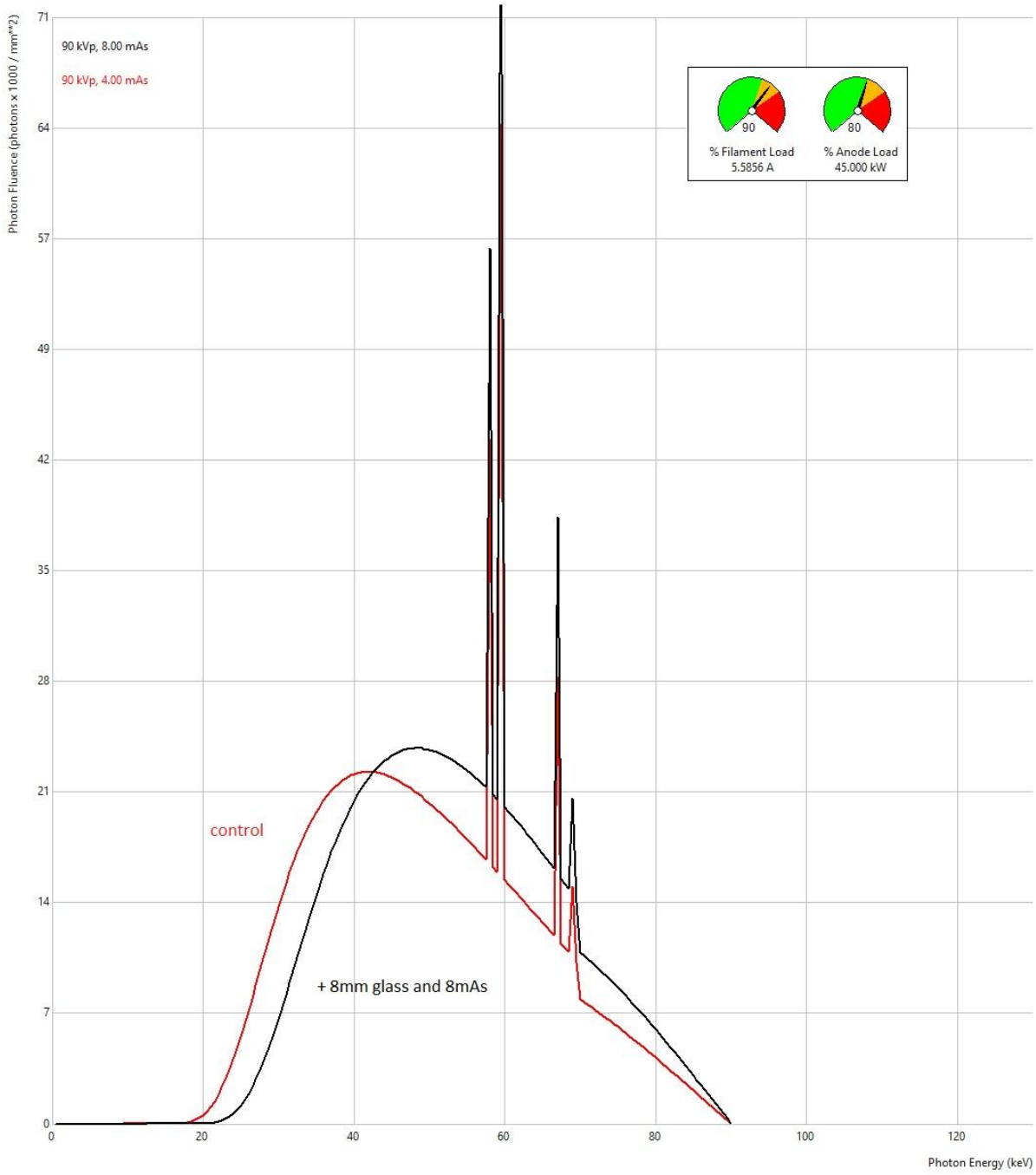

Figure 6. TechnicVR v2.0 (Shaderware Ltd, UK) simulation of the X-ray spectrum of the control beam (red line) and the experimental (black line) scenario, with increased tube charge to compensate for glass.

In the empirical physical experiment, to maintain ISAK equivalence (76.3 [0.8] μGy) when the glass window was added, the tube charge needed to be increase to 11.25 mAs, essentially a three-fold increase in output. For the experimental scenarios, when including

the glass window and using 11.25 mAs, the mean (SD) ISAK and EI were 76.3 (0.8) μGy and 182.0 (4.7), respectively. When focusing on maintaining the control zero DI, as with the original non-glass exposures. To achieve a DI of zero with the glass window in place required a tube charge 8 mAs and generated a mean (SD) ISAK and EI of 53.7 (0.1) μGy and 127.7 (3.1), respectively.

In terms of perceptual image quality, contrast sensitivity was not statistically difference between the control and experimental acquisitions (14 versus 13 discs, P=0.154). This was also similar for the evaluation of spatial resolution between the control and experimental images (17 versus 16 line pairs, P=0.540).

For the physical evaluation of SNR, CNR and spatial resolution the data are summarized in **Table 1**. Using ANOVA there was a statistically significant difference in CNR values between scenarios (P=0.005). A post-hoc Tukey analysis revealed that there was a statistically significant difference between the control (no glass) and experimental scenario 2 (glass present, target ISAK) with P=0.02. Differences between the control and experimental scenario 3 (glass present, target DI) was also statistically significant (P=0.009).

Table 1. A summary of SNR, CNR and spatial resolution results for the different scenarios.

		Mean (SD)		Spatial resolution
Scenario	**Target**	**SNR**	**CNR***	**(LP/mm)**
1 – no glass		35.5 (2.7)	2.3 (0.2)	2.24
2 – glass present	ISAK	39.6 (2.4)	1.4 (0.2)	2.50
3 – glass present	DI	37.0 (4.1)	1.2 (0.4)	2.24
*ANOVA, P=0.005.				

DISCUSSION

The novel SARS-CoV-2 coronavirus has presented unprecedented challenges to imaging departments worldwide. One of the greatest challenges is that COVID-19 is extremely contagious and there are problems in preventing cross-infection for both patients and hospital workers. It is not lost to anyone working in healthcare that there have been deaths reported in doctors, nurses and allied health professionals, including radiographers[10]. In view of this, new methods of working are essential in order to prevent disease transmission and protect both patients and staff members alike.

As part of the early response to COVID-19 practitioners at the University of Washington, in the United States, reported on the option of imaging patients directly through glass windows in isolation / side rooms[1]. Advantages of this include not requiring the practitioner to directly attend the patient's bedside and not bringing the mobile X-ray unit in close proximity to the patient. An X-ray beam directed through a glass window would normally go against standard radiographic practices, in that exposure factors would need to be modified and that there could be artefacts and image quality issues arising from such techniques. Managing COVID-19 will, however, require huge leaps of faith in how we modify our imaging practices to tackle these potential associated issues. It could be that such initiatives prove to be hugely beneficial in this fight, but at the same time they should still be subject to robust testing. Mossa-Basha and colleagues[1] describe imaging through side room windows, and state that there were no obvious image quality issues. There publication sought to describe rapid and widespread changes to their operating practices in

response to COVID-19, it is likely that image quality was not subject to the usual standard of rigorous objective testing.

Based on our initial work it can be concluded that on the basis of visual inspection, there does not appear to be any significant detriment from imaging through a glass window unit. To maintain either equivocal DI or ISAK/RIAK, the exposure factors would need to be increased by two to three-fold. This will have implications on either the wear and tear of X-ray equipment (increase in filament current) or decrease in temporal resolution (increase in exposure time) depending on how the extra charge is generated. The inclusion of a glass window within the primary beam 'hardens the beam' as seen in **Figures 5 and 6**. The reduction in low energy photons leads to a beam with a higher effective photon energy. This is likely to reduce image contrast, and this was demonstrated in the physical calculations (**Table 1**). There were no significant differences in the physical measures of SNR but there was a significant, but small, reduction in CNR when imaging through the glass window. Based on the perceptual analysis this difference was not apparent to the observers. Multiple reasons could be suggested for this, physical CNR values are much more sensitive to changes in image quality than visual inspections.[11]

This result, taken together with the possibility of reduction in temporal resolution due to the beating heart, could suggest in some instances, very subtle pathology could potentially be missed when modifying mobile imaging protocols. Many would argue that there are specific reasons for undertaking mobile radiography and that further imaging is likely when a patient's condition improves, either prior to discharge or during follow up. This however may not be the case for all patients and clinicians should be aware of the potential limitations when reviewing an X-ray image acquired through glass; as a minimum the resultant image should be annotated to reflect the modified technique.

Even for an erect patient, it is common to apply a small caudal angulation to an AP projection of the chest so that the central ray is perpendicular to the long axis of the sternum. This is to ensure the clavicles do not obscure the apices of the lungs[12]. If the patient is able to sit up erect, when using a SID of 180 cm, then this would require the center of the receptor to be approximately 20 cm below the point through which the central ray passed through the window. It can be seen that once the patient is so ill that they can only achieve a semi erect position, then a tube angulation typically of 30 degrees would be required. This would necessitate a height difference of 1 metre between the centre of the receptor and the point through which the central ray passed through the window. Since most door windows are below 180cm in height, this will require a trolley that is able to be lowered to 80cm from the floor or even less and would remain an important technical consideration.

X-raying through side room windows could have wider applicability in other areas of clinical practice where infection control is paramount. Imaging following stem cell transplantation, suspected or known cases of MRSA and clostridium difficile, to name but a few could benefit from a similar approach. Indeed, the work originally described using a similar technique by the University of Washington stemmed from the imaging of suspected Ebola virus patients in Africa[13].

Within our work, we presented the results of a novel experiment which sought to provide initial image quality and dose data regarding the practice of X-ray imaging through glass windows. Our response to modified COVID-19 radiographic techniques needed to be rapid and as such there were many additional elements to this study which could have been included. We did, however, opt to present some initial data regarding the feasibility of this

technique within other areas of practice. We do, however, agree that more work should be undertaken, including clinical analyses, before either confirming or refuting this practice definitively.

Conclusion

The response of radiology practitioners to the COVID-19 pandemic has been immense. Many new techniques and breakthroughs will result from the new knowledge and experiences gained during this time. New approaches to imaging should be carefully considered and evaluated in order to provide optimum care and safety to both staff and patients. Based on data reported with our work it does appear feasible for mobile radiography to be undertaken through side room windows in specific instances. With the potential for increases in tube output and reductions in image quality this technique should only be used when other options are not feasible, and clinicians should be aware of any modifications to standard techniques. Practitioners should also be mindful that such modifications would require additional training.

References

1. Mossa-Basha M, Medverd J, Linnau K, et al. Policies and Guidelines for COVID-19 Preparedness: Experiences from the University of Washington. *Radiology.* 2020:201326.
2. *Recommended standards for the routine performance testing of diagnostic X-ray imaging systems.* York: Institute of Physics and Engineering in Medicine; 2005.
3. Whitley AS, Clark KCPir. *Clark's positioning in radiography.* London: Hodder Arnold; 2005.
4. Sandborg M, Tingberg A, Ullman G, Dance DR, Alm Carlsson G. Comparison of clinical and physical measures of image quality in chest and pelvis computed radiography at different tube voltages. *Med Phys.* 2006;33(11):4169-4175.
5. Hess R, Neitzel U. Optimizing image quality and dose for digital radiography of distal pediatric extremities using the contrast-to-noise ratio. *Rofo.* 2012;184(7):643-649.
6. Martin C. Optimisation in general radiography. *Biomed Imaging Interv J.* 2007;3:e18.
7. Mori M, Imai K, Ikeda M, et al. Method of measuring contrast-to-noise ratio (CNR) in nonuniform image area in digital radiography. *Electronics and Communications in Japan.* 2013;96(7):32-41.
8. Inoue K, Kise K. Analysis of the Effect of Dataset Differences on Object Recognition: The Case of Recognition Methods Based on Exact Matching of Feature Vectors. *Electronics and Communications in Japan.* 2013;96(9):33-45.
9. Alves AF, Alvarez M, Ribeiro SM, Duarte SB, Miranda JR, Pina DR. Association between subjective evaluation and physical parameters for radiographic images optimization. *Phys Med.* 2016;32(1):123-132.
10. Lapolla P, Mingoli A, Lee R. Deaths from COVID-19 in healthcare workers in Italy-What can we learn? *Infect Control Hosp Epidemiol.* 2020:1-2.
11. Tapiovaara MJ. Review of relationships between physical measurements and user evaluation of image quality. *Radiation Protection Dosimetry.* 2008;129(1-3):244-248.
12. Bontrager KL, Lampignano JP. *Textbook of radiographic positioning and related anatomy.* 6th ed. / Kenneth L. Bontrager, John P. Lampignamo. ed. St. Louis, Mo. ; [London]: Elsevier Mosby; 2005.
13. Auffermann WF, Kraft CS, Vanairsdale S, Lyon GM, Tridandapani S. Radiographic Imaging for Patients With Contagious Infectious Diseases: How to Acquire Chest Radiographs of Patients Infected With the Ebola Virus. *American Journal of Roentgenology.* 2014;204(1):44-48.

Figure 1

Click here to download high resolution image

Figure 2

Click here to download high resolution image

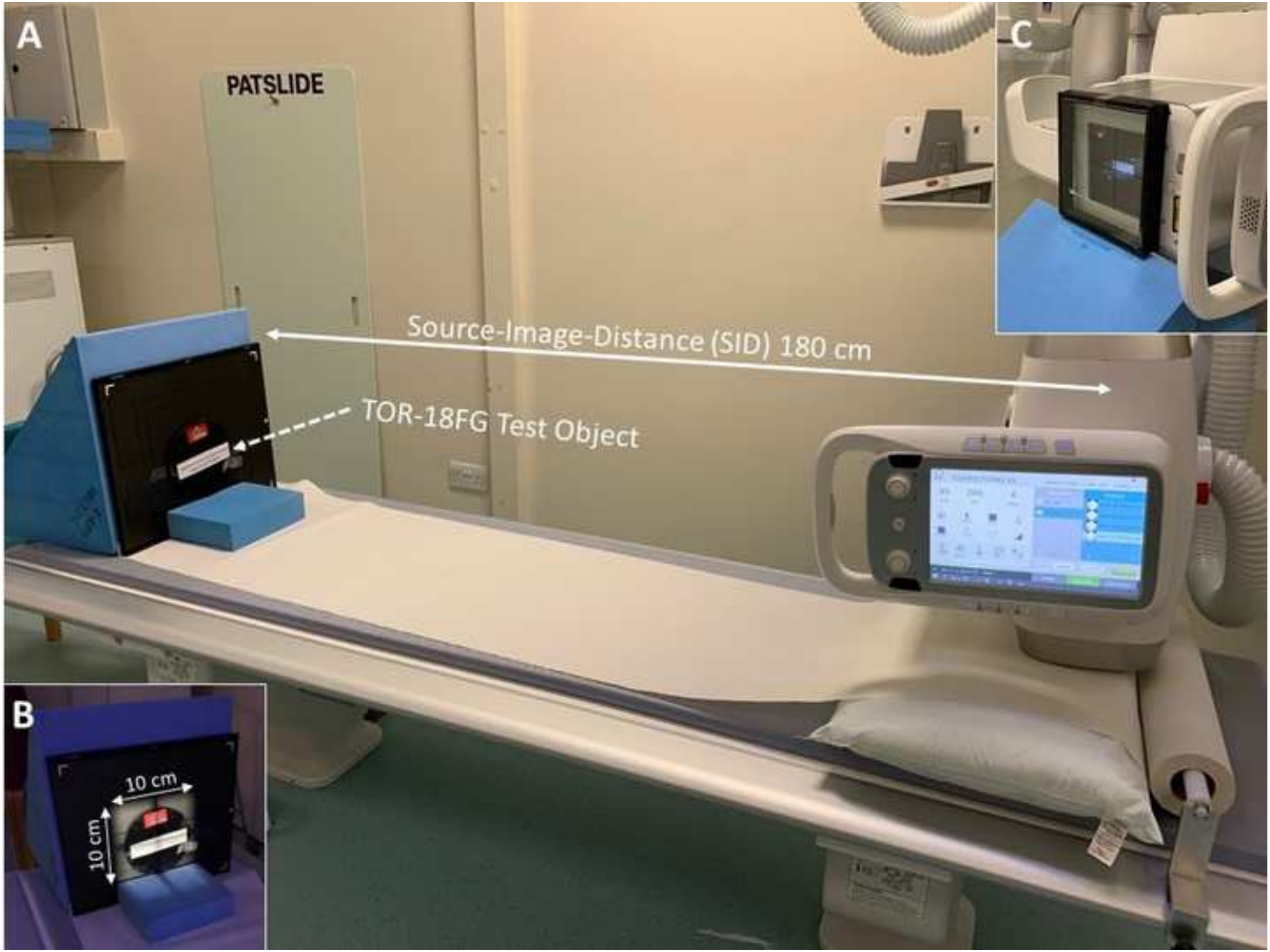

Figure 3

Click here to download high resolution image

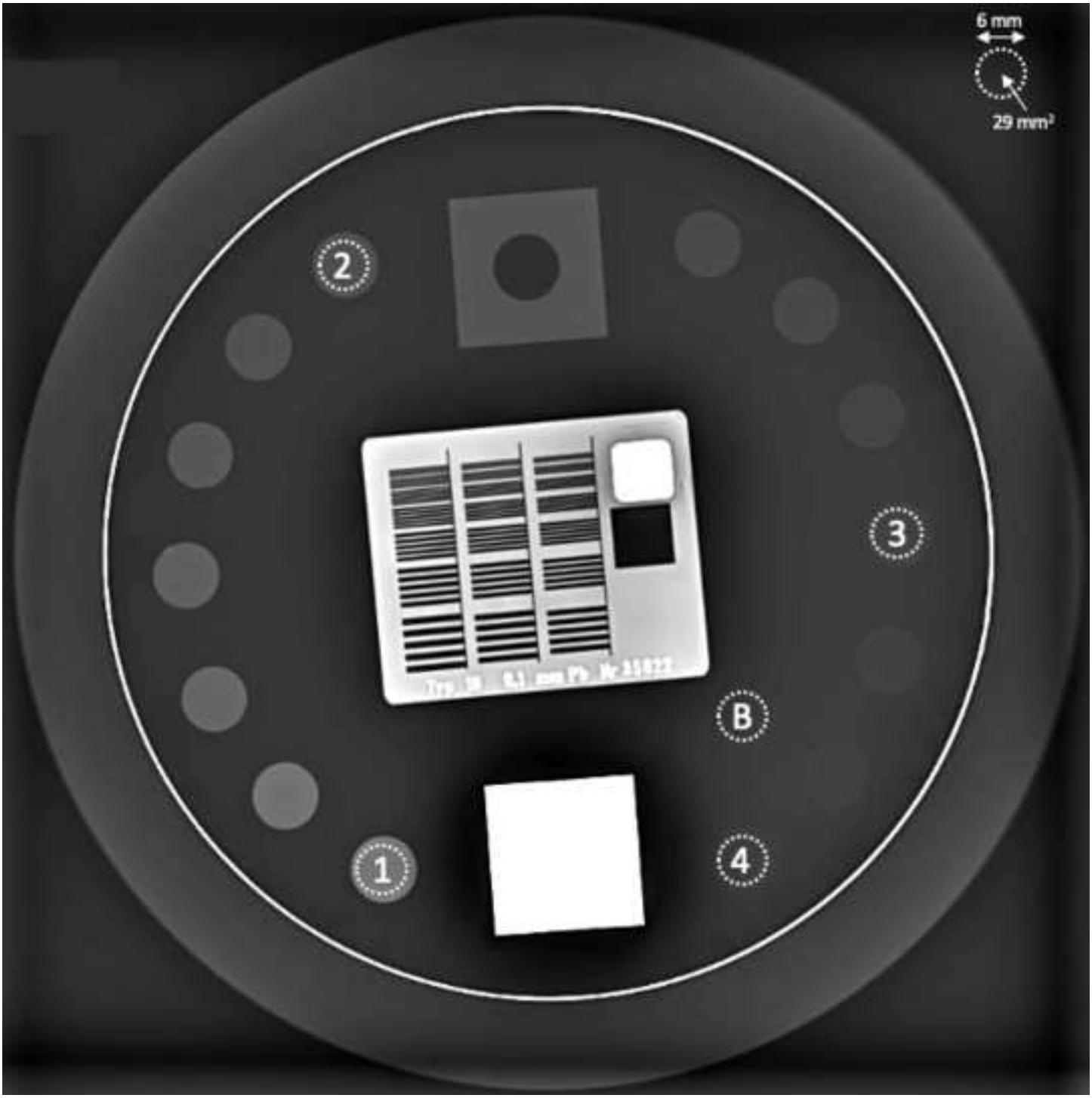

Figure 4

Click here to download high resolution image

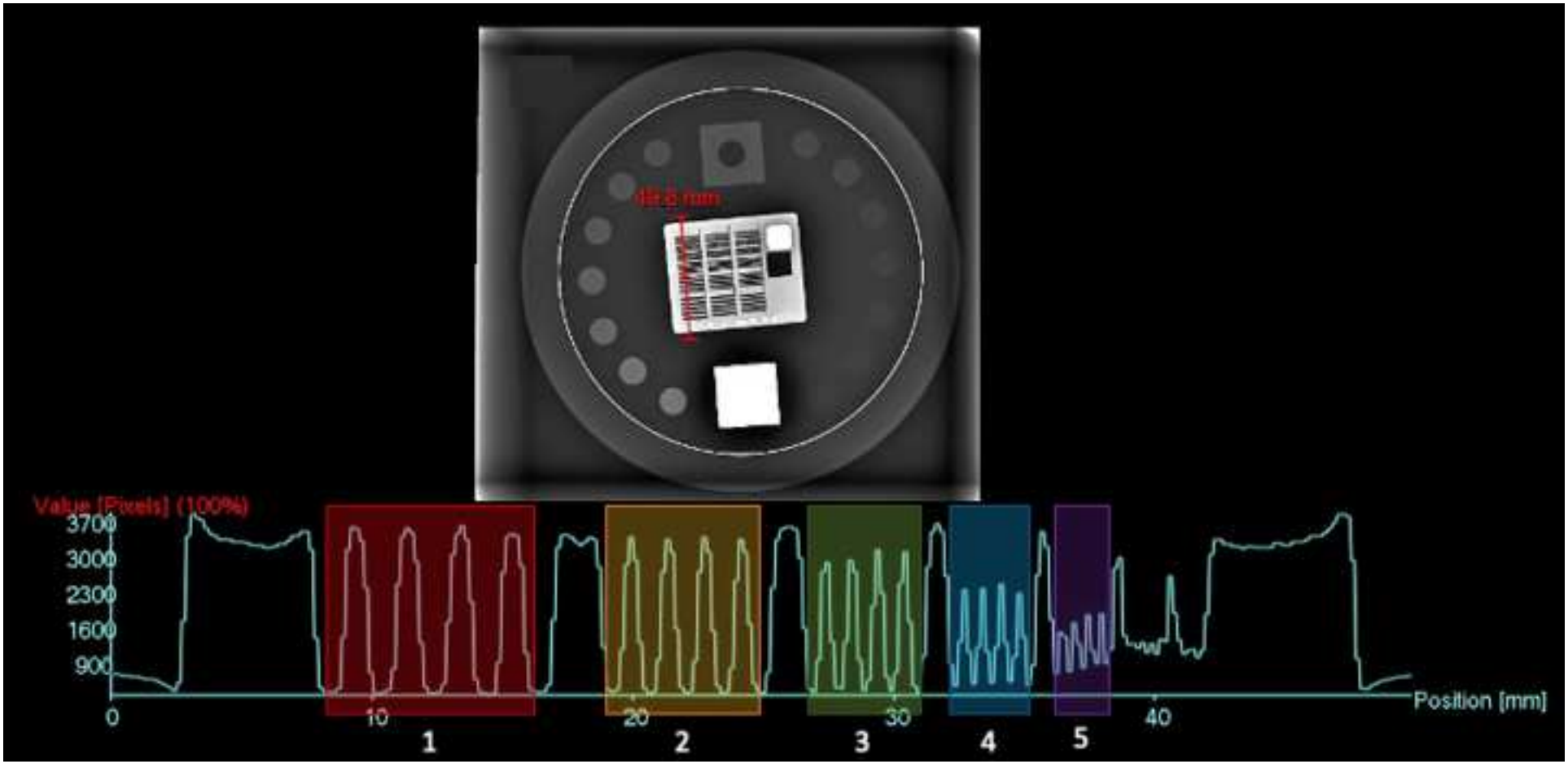

Figure 5

Click here to download high resolution image

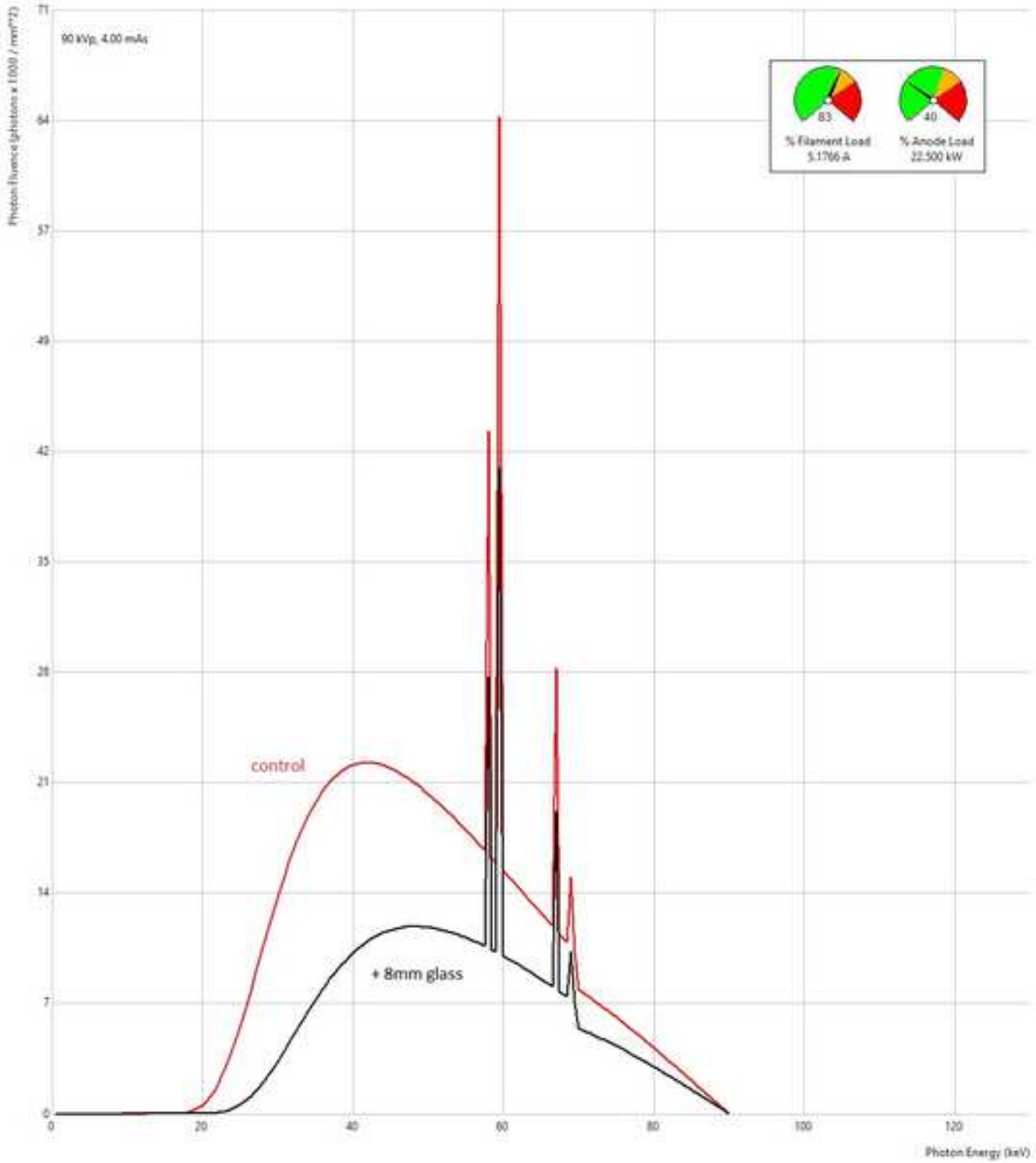

Figure 6

Click here to download high resolution image

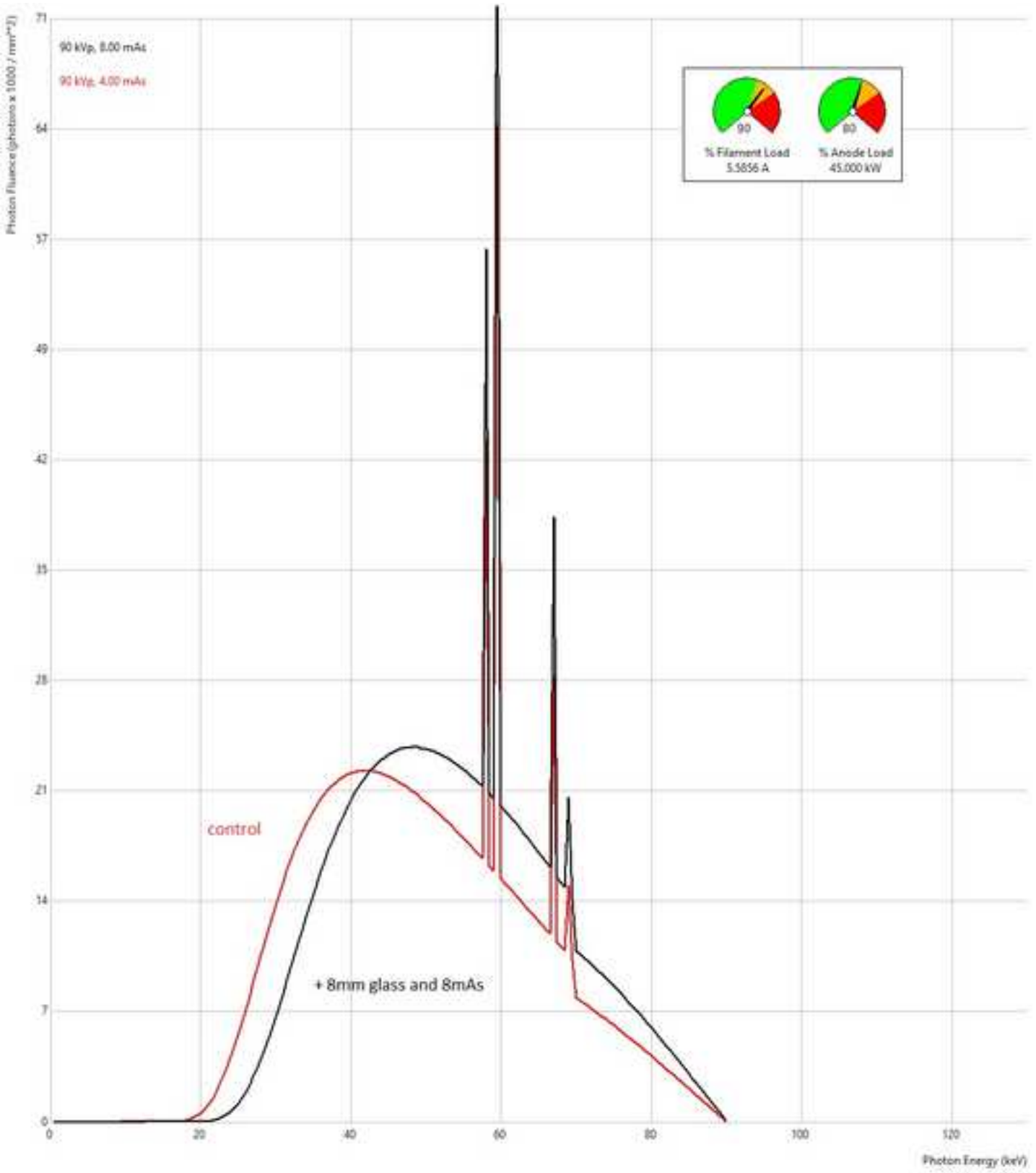

Table(s)

Table 1. A summary of SNR, CNR and spatial resolution results for the different scenarios.				
		Mean (SD)		**Spatial resolution (LP/mm)**
Scenario	**Target**	**SNR**	**CNR***	
1 – no glass	[redacted]	35.5 (2.7)	2.3 (0.2)	2.24
2 – glass present	ISAK	39.6 (2.4)	1.4 (0.2)	2.50
3 – glass present	DI	37.0 (4.1)	1.2 (0.4)	2.24
*ANOVA, P=0.005.				